ELSEVIER

PII: S0032-3861(96)00948-2

Polymer Vol. 38 No. 15, pp. 3745–3752, 1997

0032-3861/97/$17.00+0.00

Morphology and phase behaviour of poly(methyl methacrylate)/poly(styrene-*co*-acrylonitrile) blends monitored by *FT*i.r. microscopy

Rüdiger Schäfer, Jörg Zimmermann, Jörg Kressler* and Rolf Mülhaupt
Institut für Makromolekulare Chemie und Freiburger Materialforschungszentrum, Albert-Ludwigs-Universität Freiburg, Stefan-Meier-Strasse 21, D-79104 Freiburg i. Br., Germany
(Received 31 July 1996)

It has been shown that Fourier transform infrared (*FT*i.r.) microscopy is able to monitor the phase morphology in blends of poly(methyl methacrylate) and poly(styrene-*co*-acrylonitrile). This is carried out by the spatially resolved detection of the absorbances of the C=O stretching vibration of the ester group of poly(methyl methacrylate) at 1732 cm^{-1} and the C≡N stretching vibration of poly(styrene-*co*-acrylonitrile) at 2238 cm^{-1}. The most serious restriction for *FT*i.r. microscopy is the large i.r. spot size which limits the spatial resolution of the detectable morphologies. An enormous advantage of *FT*i.r. microscopy compared to optical microscopy is its ability to provide quantitative information on the chemical composition of the phases. These data taken at different annealing temperatures can be used to obtain the phase diagram of blends showing lower critical solution temperature behaviour. Larger deviations of data points measured by *FT*i.r. microscopy compared to cloud point measurements are observed at the poly(methyl methacrylate)-rich side of the phase diagram, where also the error of the *FT*i.r. microscopic determination of the phase composition is larger for the blend system under investigation. © 1997 Elsevier Science Ltd.

(Keywords: *FT*i.r. microscopy; morphology; polymer blends)

INTRODUCTION

The polymer blend system poly(methyl methacrylate)/poly(styrene-*co*-acrylonitrile) (PMMA/PS-*co*-AN) has been studied widely by several experimental techniques[1–5]. One of the main reasons to investigate this blend system is the occurrence of a miscibility window, i.e. simply by varying the copolymer composition of PS-*co*-AN the miscibility with PMMA can be adjusted[6–9]. Polymer blends containing PS-*co*-AN with 9–34 wt% of acrylonitrile are miscible at room temperature and show lower critical solution temperature (LCST) behaviour upon heating at the edges of the miscibility window. Thus the effective interaction parameter between PMMA and PS-*co*-AN can be varied simultaneously with related quantities such as diffusion coefficients[10], interfacial thickness[11,12] and adhesion[13,14]. Also, the large difference in the refractive indices between PMMA and PS-*co*-AN makes this blend system suitable for studies using optical methods.

It has been shown that *FT*i.r. microscopy (sometimes referred to as *FT*i.r. microspectroscopy) is a suitable tool to analyse multicomponent systems qualitatively and quantitatively[15]. In the beginning, mainly large defects up to about 150 μm or fibres embedded in a polymeric matrix as well as biological systems were detected and spatially resolved[15–18]. *FT*i.r. microscopy was later used for the mapping of different polymeric multiphase systems[19–22].

* To whom correspondence should be addressed

The aim of this paper is to use *FT*i.r. microscopy to monitor the phase morphology of PMMA/PS-*co*-AN blends. Instead of different refractive indices which allow the observation of the phase morphology by optical microscopy, *FT*i.r. microscopy monitors characteristic i.r. bands of the respective spatially resolved blend components. For the blend system under investigation it is most suitable to study the spatial distribution of the intensity of the carbonyl vibration which belongs to PMMA and of the nitrile vibration connected with the acrylonitrile in PS-*co*-AN, respectively. Additionally, the chemical composition of the phases can be recorded quantitatively as a function of annealing temperature, thus providing the possibility of obtaining phase diagrams.

EXPERIMENTAL

Materials

A PS-*co*-AN random copolymer with 30.5 wt% of acrylonitrile was used for most of the measurements (PS-*co*-AN-30.5). The M_w value of PS-*co*-AN-30.5 was 186 000 g mol^{-1}, and M_w/M_n was about 2. The PMMA sample had an M_w value of 43 000 g mol^{-1}, and M_w/M_n was about 1.7[6]. For the preparation of a bilayer specimen a PS-*co*-AN with 38.7 wt% of acrylonitrile was used (PS-*co*-AN-38.7). This sample had an M_w value of 181 000 g mol^{-1}, and M_w/M_n was about 2. The glass transition temperatures of all polymers were in the range between 100 and 120°C[6]. The synthesis of all samples is described elsewhere[6].

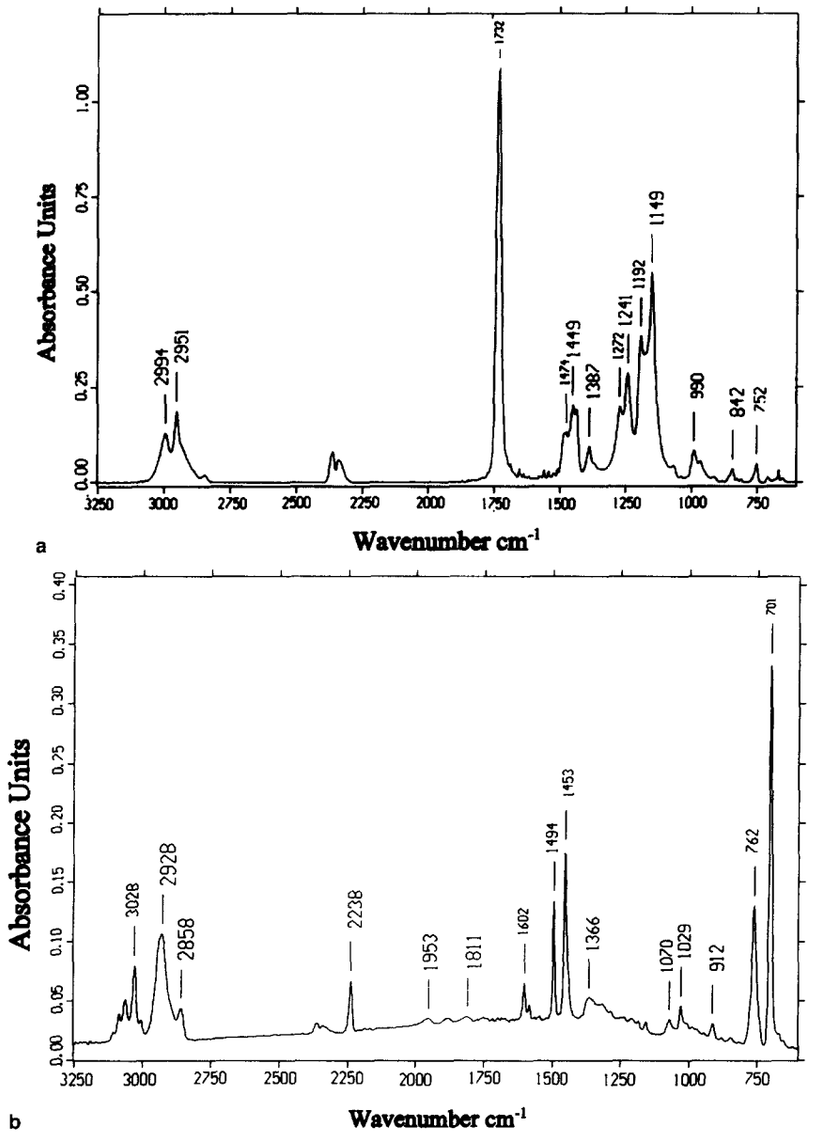

Figure 1 *FT* i.r. spectra of the neat polymers at room temperature: (a) PMMA and (b) PS-*co*-AN-30.5

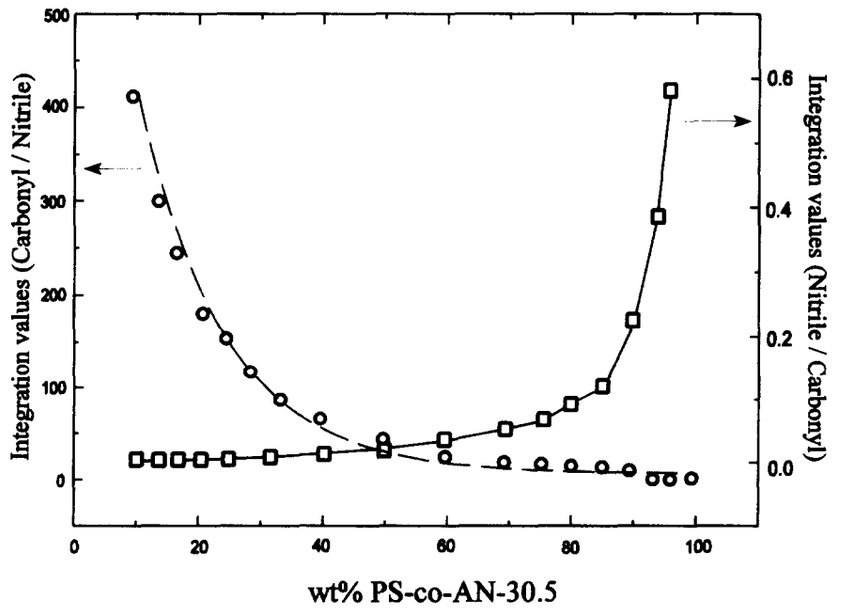

Figure 2 The calibration curve shows the ratio of the integration value of the carbonyl peak to the nitrile peak and vice versa as a function of the amount of PS-*co*-AN-30.5 in the blends

Sample preparation for FT*i.r. and light microscopy*

For the mapping of the morphology and the determination of the phase diagram by *FT*i.r. microscopy, a total 5 wt% of polymer containing 60 wt% of PS-*co*-AN-30.5 and 40 wt% of PMMA was dissolved in tetrahydrofuran. This solution was cast onto KBr plates. These samples were dried at room temperature in vacuum and then annealed for different periods of time at different temperatures. For the determination of the calibration curve different blend ratios were prepared and annealed at 50°C in vacuum. Then the ratios of the integration values of the carbonyl and nitrile peaks were determined and used for the calibraton curve.

For the preparation of a bilayer specimen, a plate of PMMA and PS-*co*-AN-38.7, respectively, with a thickness of 2 mm was prepared in a hot press at 190°C for 5 min between high-gloss metal plates. The two polymer plates were mounted together and isothermally annealed at 190°C for 42 h. The bilayer specimen was cut perpendicular to the surface into two pieces. Then a thin section with the thickness of about 3 μm was microtomed at room temperature.

For the light microscopic determination of the phase diagram of PMMA/PS-*co*-AN blends, eight different solutions with different polymer blend ratios were prepared and cast onto glass plates. These samples were slowly heated on a hot stage at 0.2°C min^{-1}. The cloud points were then determined by microscopic inspection.

FT*i.r. microscopy*

The i.r. spectra were recorded on a Bruker IFS 88 *FT*i.r. spectrometer coupled with an i.r. microscope and equipped with a computer-controlled *XY* mapping stage. An MCT detector in the transmission mode was used. The mapping conditions used for recording the i.r. spectra were as follows: a 36× Cassegrain objective coupled with a 15× condenser and an aperture of diameter 0.6 mm, 500 scans for signal averaging at a resolution of 4 cm^{-1}, 5 or 10 μm step size in the *X* and *Y* directions with a 90 × 90 μm total size. Taking into consideration diffraction effects[15,22] leads to an average spot size of 25 μm. The spot size was checked by measuring the absorbance of a polyethylene peak at 2920 cm^{-1} across a sharp boundary (polyethylene foil/air)[23]. In order not to approach the diffraction limit of *FT*i.r. microscopy, which is with this combination of apertures below 1000 cm^{-1}, the carbonyl band of PMMA

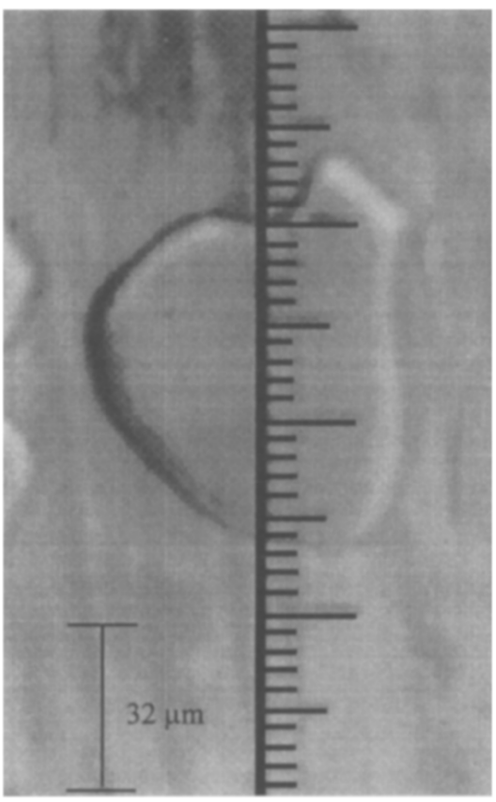

a

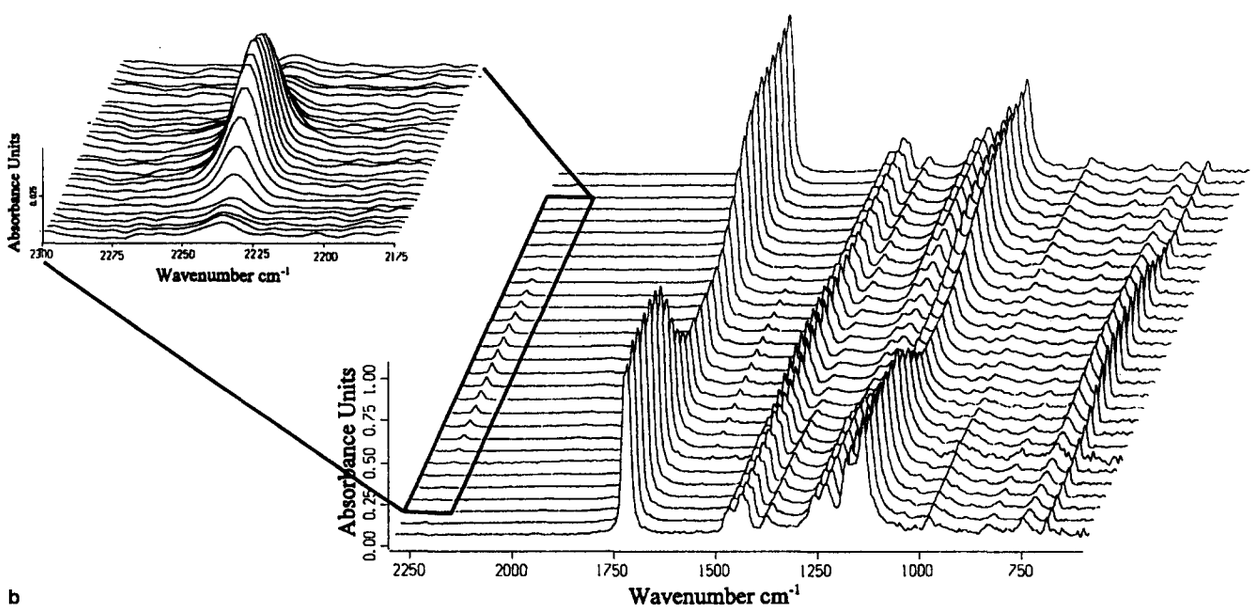

b

Figure 3 (a) Light micrograph of the morphology of PS-*co*-AN-30.5/PMMA blends after phase separation at 210°C for 510 min. (b) Spatially resolved *FT*i.r. spectra are taken along the scale bar indicated in *Figure 3a*. The step size is 5 μm

at 1732 cm^{-1} and the nitrile band of PS-*co*-AN at 2238 cm^{-1} were used for morphology mapping. Parfocal and colinear with the i.r. radiation was a visible optical train[15]. Optical images were obtained with a charge-coupled device (CCD) camera equipped to the i.r. microscope using a 15×objective for magnification.

RESULTS AND DISCUSSION

Figure 1 shows the spectra of the respective neat components. Most suitable for a quantitative evaluation of PMMA is the C=O stretching vibration of the ester group at 1732 cm^{-1} which can be seen in the spectrum of

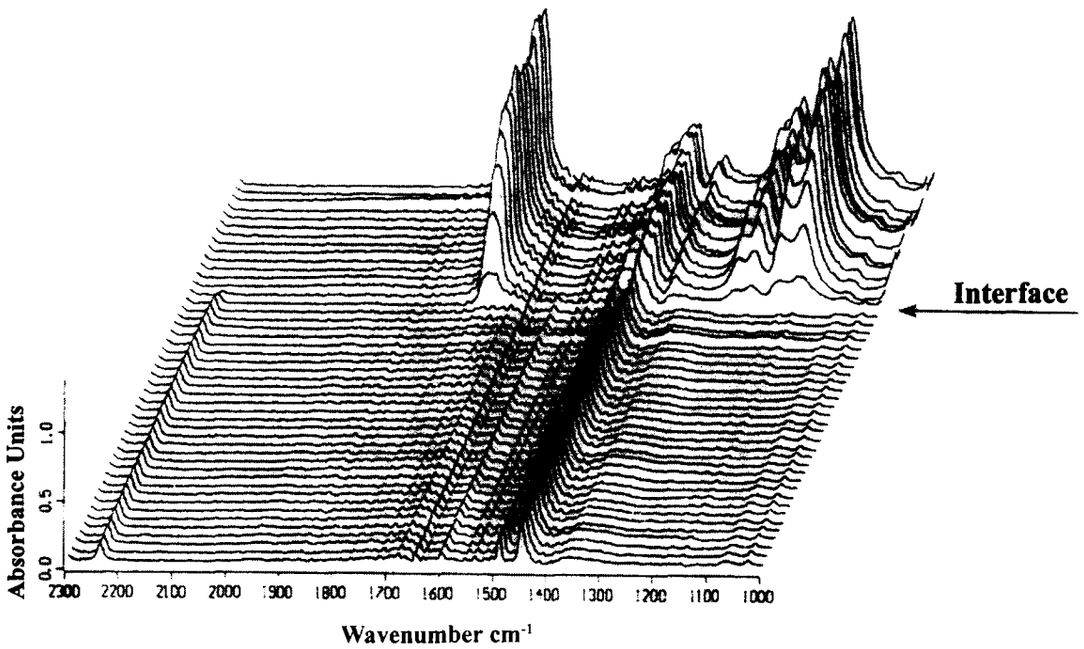

Figure 4 Spatially resolved *FT* i.r. spectra taken across the interface of a bilayer specimen of PMMA/PS-*co*-AN-38.7. The step size is 5 μm

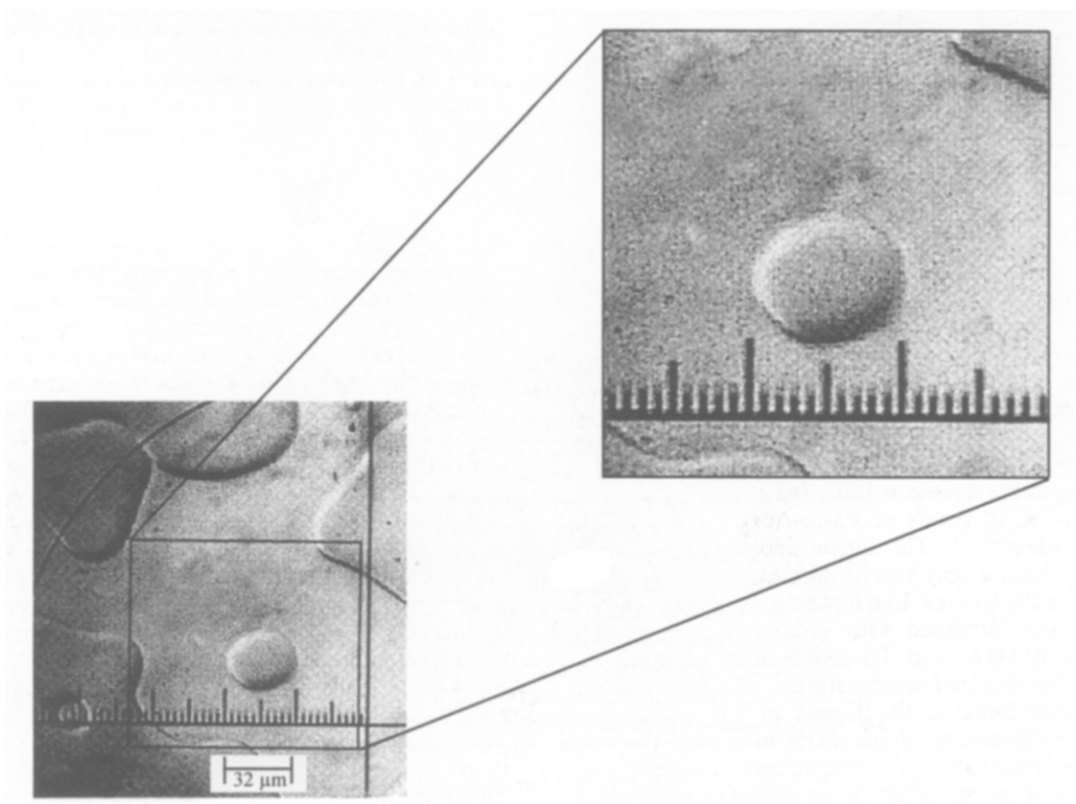

Figure 5 Light micrograph of the scanning area used for *FT* i.r. microscopy. The PS-*co*-AN-30.5/PMMA (60/40 wt%) is annealed for 510 min at 190°C

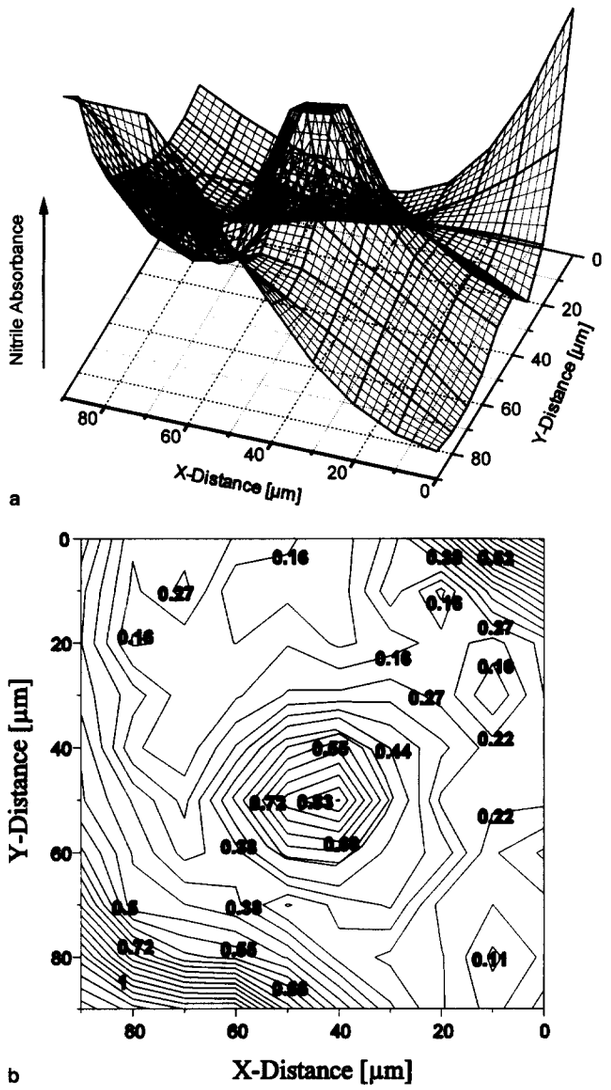

Figure 6 Functional group image of the nitrile peak of the area shown in *Figure 5* represented by (a) the axonometric plot and (b) the corresponding contour plot

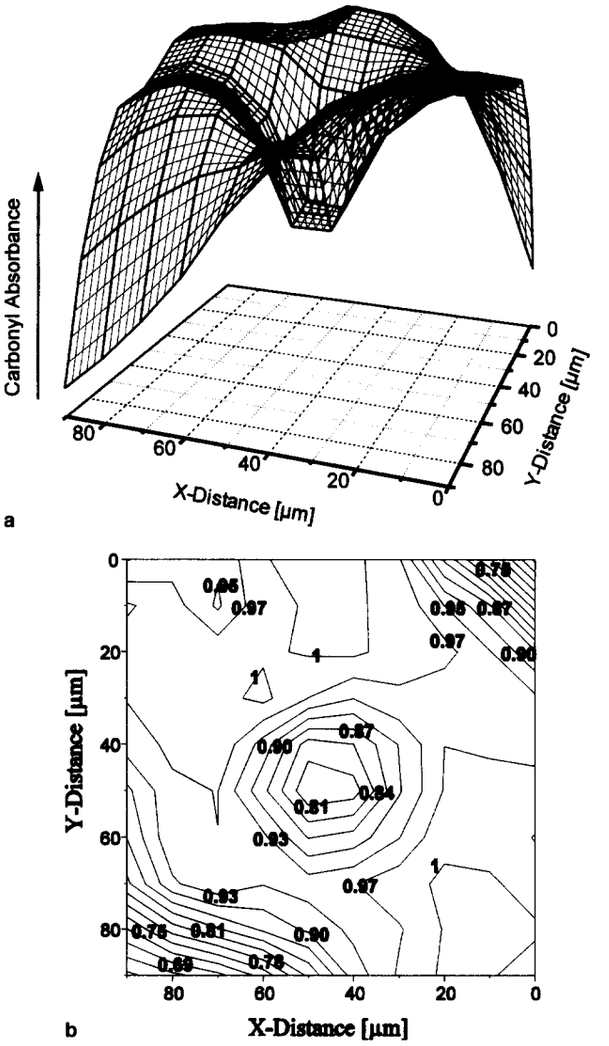

Figure 7 Functional group image of the carbonyl peak in the area shown in *Figure 5* represented by (a) the axonometric plot and (b) the corresponding contour plot

Figure 1a. Other characteristic bands of PMMA which do not appear in the PS-*co*-AN spectrum are the stretching vibrations of C–O–C which are split in the range from 1272 to 1149 cm^{-1} [24]. For a quantitative evaluation of the PS-*co*-AN content of the phases, the C≡N vibration at 2238 cm^{-1} is most suitable (see *Figure 1b*). Other characteristic bands of PS-*co*-AN which do not interfere with the PMMA spectrum are caused by the phenyl ring of the styrene at 1602, 762 and 701 cm^{-1}. The assignment of all bands of PS-*co*-AN is given in full detail elsewhere[25–27]. The nitrile and carbonyl bands mentioned belong only to one species and appear well separated in the spectra. In a first step, blends of the two polymers were prepared with a different blend ratio. Blends of PMMA and PS-*co*-AN-30.5 show LCST behaviour at elevated temperatures[6]. But keeping the solution cast films of the blends at sufficiently low temperatures generates single-phase mixtures. Thus by varying the blend ratio, a calibration curve can be drawn, as shown in *Figure 2*. Here the ratio of the integration value of the nitrile to the carbonyl peak and vice versa is shown as a function of the PS-*co*-AN-30.5 content of the blend. Thus a quantitative analysis of the chemical composition of the different phases is always possible by using the calibration curves.

Now, the polymer morphology can be studied quantitatively. *Figure 3* shows measurements which are necessary in order to obtain the blend morphology by *FT*i.r. microscopy. *Figure 3a* depicts for comparison a morphology obtained by light microscopy. The PS-*co*-AN-30.5/PMMA (60/40 wt%) blend was isothermally annealed at 210°C for 510 min. Thus the blend is transferred into the two-phase region above the LCST. The phase separation in the PS-*co*-AN-30.5/PMMA blends occurs via spinodal decomposition, as studied extensively in the literature[28]. In the late stage of phase separation the co-continuous phase morphology coarsens, and large separated droplets appear[29]. Thus the different phases reach a size which can be monitored by *FT*i.r. microscopy. *Figure 3b* depicts an *FT*i.r. scan taken along the scale bar shown in *Figure 3a* starting at the lower part of the photograph. Using these data, it is possible to obtain information on the chemical composition of the phases. It can be seen that the scan starts in the PMMA-rich phase. The C=O band at 1732 cm^{-1} has a strong

absorbance. Furthermore, the absorbances of the C–O–C bands in the range from 1272 to 1149 cm^{-1} and of the bands caused by the α-methyl group of the PMMA at 990 and 1387 cm^{-1} are stronger compared to that in the area of the droplet shown in *Figure 3a*. But the phenyl ring vibrations at 701 and 762 cm^{-1} appear also in this phase, thus showing that a mixed phase is formed. The major component of this phase is PMMA, and the minor component is PS-*co*-AN-30.5. Also, the band caused by the phenyl ring at 1602 cm^{-1} and the nitrile band at 2238 cm^{-1} can be detected in the PMMA-rich phase. This is demonstrated for the C≡N band in the enlarged area of *Figure 3b*. This enlargement is necessary because the absorbance of this band is much weaker compared to that of the carbonyl band. Moving the i.r. spot with a step size of 5 μm along the scale bar shown in *Figure 3a* leads to a point where the absorbance of the C=O vibration (and all bands caused by PMMA) starts to decrease and simultaneously the C≡N vibration (and bands which belong to PS-*co*-AN-30.5) starts to increase.

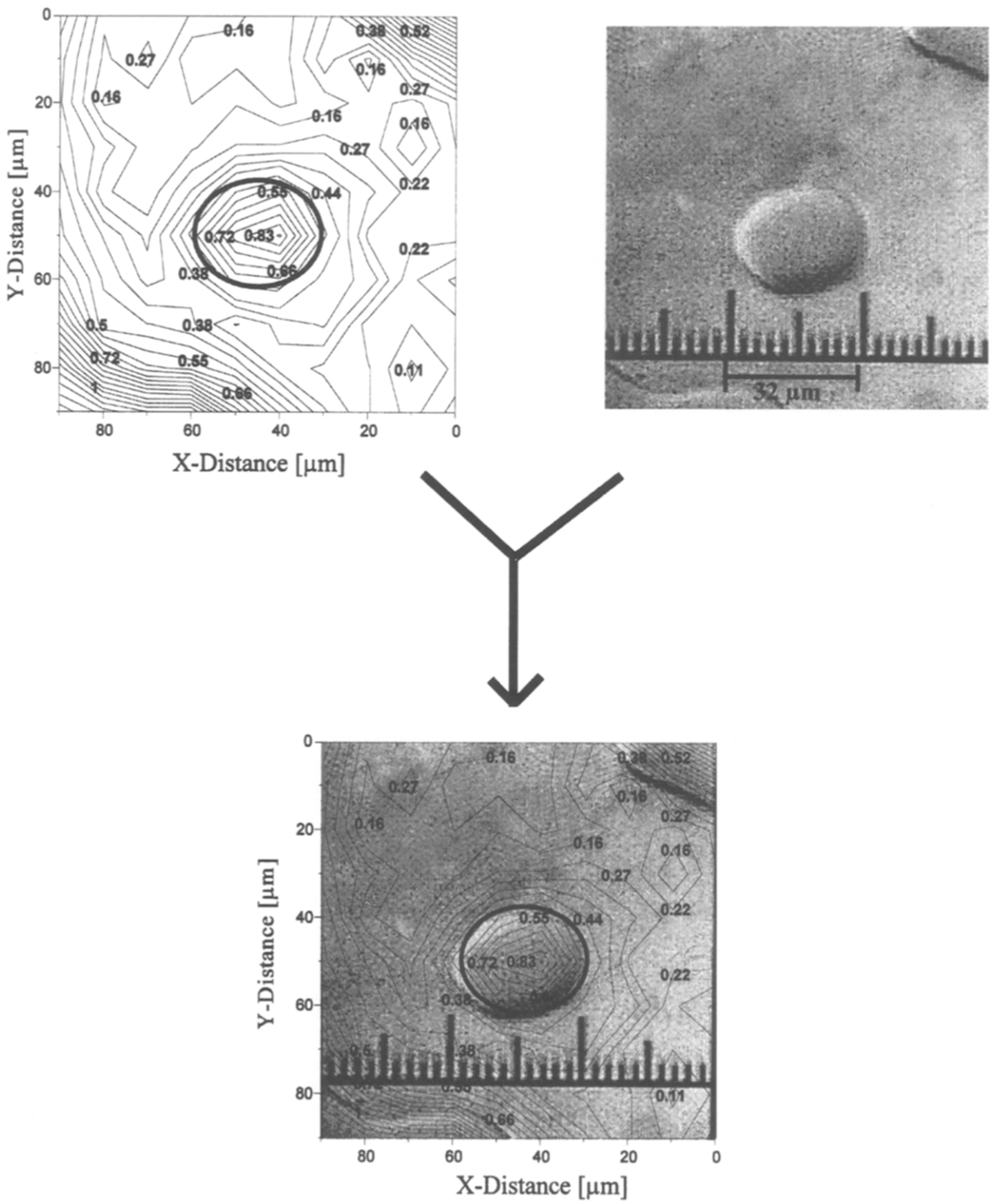

Figure 8 Comparison of light microscopy and *FT* i.r. contour plot of the nitrile band for the same system as discussed in *Figures 5–7* (see text)

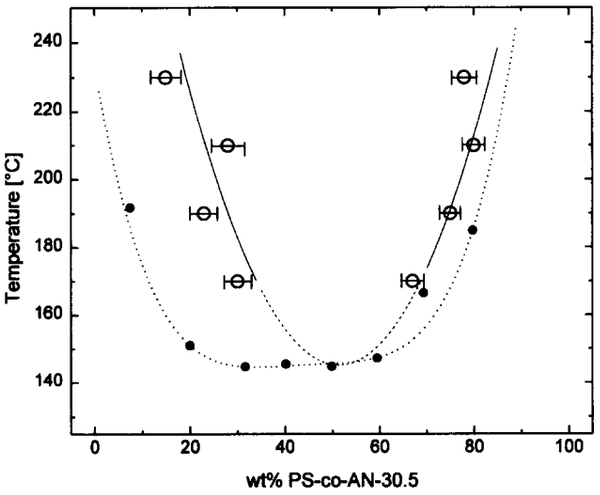

Figure 9 Cloud points obtained by light microscopy (●) and the phase composition obtained by *FT* i.r. microscopy (○). The lines represent the best fit to guide the eye

Thus the PS-*co*-AN-30.5-rich phase can be seen. It also contains bands due to PMMA. The quantitative composition of the phases can be obtained using the calibration curves as demonstrated below. Thus the comparison with the light micrograph of *Figure 3a* leads to the result that the droplets represent the PS-*co*-AN-30.5-rich phase surrounded by a PMMA-rich matrix. Furthermore, it can be seen that there is an apparently broad transition zone of about 25 μm between the PMMA-rich and the PS-*co*-AN-rich phases. There are always five spectra taken in steps of 5 μm where the absorbance decreases or increases before reaching a plateau region. However, it is known that the interfacial thickness in the polymer blend system is usually in the range of several nanometres[29,30]. Thus the apparent broadening at the phase borders is mainly a result of the i.r. spot size (25 μm). This is demonstrated in *Figure 4*, where *FT* i.r. microscopy is employed for bilayer specimens of PS-*co*-AN-38.7 and PMMA. These two polymers are immiscible, and their interfacial thickness is only about 30 nm[11,12]. This interfacial thickness is obviously negligible compared to the broadening of the concentration profiles caused by the spot size of the i.r. beam. The spectra in the front of *Figure 4* belong to the bulk phase of PS-*co*-AN-38.7 and that in the back to PMMA. The transition from one plateau region to the other takes also about five spectra, i.e. 25 μm. Therefore, it can be assumed that the real interface is located exactly in the middle between the five spectra of the transition region where the absorbance changes. Using this information it is now possible to monitor the morphology by *FT* i.r. microscopy quantitatively.

The optical micrograph of *Figure 5* shows the area of the sample used for *FT* i.r. microscopy. This morphology is obtained for a PS-*co*-AN-30.5/PMMA blend (60/40 wt%) isothermally annealed for 510 min at 190°C. The i.r. images of the scanned area are shown in *Figure 6*. The functional group image of the C≡N group is represented by the axonometric as well as the contour plots. The axonometric image shows the C≡N absorbance spatially resolved and the contour plot shows the iso-absorbance lines. The centre of the image and the upper right as well as the lower left part of the image show the PS-*co*-AN-enriched domains. In these areas the absorbance of the nitrile band is stronger compared to the other areas of the sample. According to the key–lock principle these areas must contain less PMMA than the surrounding areas. This is demonstrated in *Figure 7*, where the C=O band is shown spatially resolved. In the areas enriched with PS-*co*-AN-30.5, the carbonyl absorbance is significantly lower. In order to obtain the real morphology from i.r. microscopic measurements shown in *Figures 6* and *7*, it is now necessary to take into account the apparent broadening of the interface measured for the bilayer specimen. This procedure is demonstrated in *Figure 8*. The two upper pictures show the contour plot of the C≡N vibration and the corresponding light micrograph as shown in *Figures 5* and *6b*. Taking into consideration the fact that the real phase boundary is located in the middle of the apparent concentration profile changes the gradual concentration profile at the interface to a nearly step function. This is represented by the bold, full line in the contour plot. This is now identical with the optical image. It should be mentioned that the curvature of the droplet leads also to an apparent broadening. But the sample thickness (about 3 μm) is much smaller compared to the droplet size. Therefore, the effect of the curvature is relatively small. Furthermore, microtomed bulk samples are used to compare the results obtained for cast and annealed films. Both types of measurements show the same results.

As already discussed, it is possible to determine the chemical composition of the phases exactly using the calibration curves shown in *Figure 2*. These measurements are basically suitable to obtain the phase diagram of PMMA/PS-*co*-AN-30.5 blends which show LCST behaviour. In order to determine the phase diagram different blend ratios are usually prepared and heated[32]. The cloud points are then taken by microscopic measurements. The phase diagram obtained by this method is shown in *Figure 9*. But additionally the blends were isothermally annealed for a time, which generates phase sizes large enough in order to probe the chemical composition of the phases by *FT* i.r. microscopy. Then in the plateau regions, i.e. in an area where the i.r. spot probes exclusively one phase, the absorbances of the carbonyl and nitrile bands are measured. Using the calibration curve allows the determination of the chemical composition of the phases. These values are also shown in *Figure 9*. The values represent the average of at least five different measurements at different spots. It can be seen that the error is larger in the PMMA-rich region because the absorbance of the nitrile band is relatively weak there. Using this method it is possible to obtain the phase diagram sufficiently far away from the critical point. Near to the critical point the growth of the phases is too slow to allow the phase sizes necessary for a quantitative evaluation by *FT* i.r. microscopy to be obtained.

CONCLUSIONS

It has been shown that *FT* i.r. microscopy is a suitable tool to monitor polymer blend morphologies. Its main advantage compared to optical microscopy is the possibility to determine the chemical composition of the respective domains quantitatively. A disadvantage is the limited resolution of *FT* i.r. microscopy, which depends on the experimental set-up and the wavelength of the vibration of the functional group detected. But,

generally speaking, the domain sizes detected should be at least 10 μm. The monitoring of the chemical composition of the different phases as a function of the annealing temperature can be used in order to construct a phase diagram. This phase diagram is slightly narrower compared to that obtained by cloud point measurements. The data points obtained by *FT*i.r. microscopic as well as light microscopic measurements are in good agreement at the PS-*co*-AN-30.5-rich side of the phase diagram. The agreement for the PMMA-rich side is relatively poor because of the small absorbance of the nitrile band compared to the carbonyl band, which yields a larger error of the data points in this region. But, basically, *FT*i.r. microscopy is able to monitor phase compositions as a function of temperature, thus providing the possibility of establishing phase diagrams. *FT*i.r. microscopy might in the future also be a suitable tool to monitor blend morphologies in which both components have a similar refractive index as, for example blends of a polymer with its deuterated analogue.

ACKNOWLEDGEMENT

Financial support was given by the Deutsche Forschungsgemeinschaft (SFB 60).

REFERENCES

1. Stein, D. J., Jung, R. H., Illers, H. H. and Hendus, H., *Angew. Makromol. Chem.*, 1974, **36**, 89.
2. Frezotti, D. and Ravanetti, G. P., *J. Therm. Anal.*, 1994, **41**, 1237.
3. Yang, H. H., Han, C. D. and Kim, J. K., *Polymer*, 1994, **35**, 1503.
4. Qultache, A. K., Zhao, Y., Jasse, B. and Monnerie, L., *Polymer*, 1994, **35**, 681.
5. Ho, T. and Mijovich, J., *Macromolecules*, 1990, **23**, 1411.
6. Suess, M., Kressler, J. and Kammer, H. W., *Polymer*, 1987, **28**, 957.
7. Nishimoto, N., Keskkula, H. and Paul, D. R., *Polymer*, 1989, **30**, 1279.
8. Cowie, J. M. G., Reid, V. M. C. and McEwen, I. J., *Polymer*, 1990, **31**, 486.
9. Higashida, N., Kressler, J. and Inoue, T., *Polymer*, 1995, **36**, 2761.
10. Kim, E., Kramer, E. J., Wu, W. C. and Garrett, P. D., *Polymer*, 1994, **35**, 1332.
11. Higashida, N., Kressler, J., Yukioka, S. and Inoue, T., *Macromolecules*, 1992, **25**, 5259.
12. Kressler, J., Higashida, N., Inoue, T., Heckmann, W. and Seitz, F., *Macromolecules*, 1993, **26**, 2090.
13. Willett, J. L. and Wool, R. P., *Macromolecules*, 1993, **26**, 5336.
14. Cho, K. O., Kressler, J. and Inoue, T., *Polymer*, 1994, **35**, 1332.
15. Messerschmidt, R. G. and Harthcock, M. A., *Infrared Microspectroscopy: Theory and Applications*. Marcel Dekker, New York, 1988.
16. Harthcock, M. A., Lentz, L. A., Davis, B. L. and Krishnan, K., *Appl. Spectrosc.*, 1986, **40**, 210.
17. Harthcock, M. A. and Atkin, S. C., *Appl. Spectrosc.*, 1988, **42**, 449.
18. Dalterio, R. A., Ticknor, A. B., Combs, C. M., Moon, S. L. and Rosenberg, I. E., *Appl. Spectrosc.*, 1990, **44**, 1575.
19. Mizakoff, B., Taga, K. and Keller, R., *Appl. Spectrosc.*, 1993, **47**, 1476.
20. McFarland, C. A., Koenig, J. L. and West, J. L., *Appl. Spectrosc.*, 1993, **47**, 321.
21. Challa, S. R., Wang, S. Q. and Koenig, J. L., *Appl. Spectrosc.*, 1995, **49**, 267.
22. Sommer, A. J. and Katon, J. E., *Appl. Spectrosc.*, 1991, **45**, 1633.
23. Schäfer, R., Kressler, J., Neuber, R. and Mülhaupt, R., *Macromolecules*, 1995, **28**, 5037.
24. Hummel, D. and Scholl, F., *Atlas der Kunststoffanalyse*. Hanser, Munich, 1968.
25. Nyquist, R. A., *Appl. Spectrosc.*, 1987, **41**, 797.
26. Nyquist, R. A., *Appl. Spectrosc.*, 1984, **38**, 264.
27. Krimm, S., *Fortschr. Hochpolym. Forsch.*, 1960, **2**, 140.
28. Maruta, J., Ohnaga, T. and Inoue, T., *Macromolecules*, 1993, **26**, 6386.
29. Hashimoto, T., in *Material Science and Technology*, ed. R. W. Hahn, P. Haasen and E. J. Kramer. VCH, Weinheim, 1993.
30. Broseta, D., Fredrickson, G. H., Helfand, E. and Leibler, L., *Macromolecules*, 1990, **23**, 132.
31. Sanchez, I. C. (ed.) *Physics of Polymer Surfaces and Interfaces*. Butterworth-Heinemann, Stoneham, MA, 1992.
32. Kressler, J., Kammer, H. W. and Klostermann, K., *Polym. Bull.*, 1986, **15**, 113.